Check for updates

Geophysical Research Letters

RESEARCH LETTER
10.1029/2025GL117927

Implications for Oceanographic and Seafloor Geodetic Applications Due To Settling of Self-Calibrating Bottom Pressure Recorders

Nicholas Harmon[1,2], Catherine A. Rychert[1,2], Ben Moat[3], David Smeed[3], Eleanor Frajka-Williams[4], Tillys Petit[3], Martin Walker[5], Paul Provost[3], and Tina Thomas[3]

[1]Woods Hole Oceanographic Institution, Woods Hole, MA, USA, [2]University of Southampton, Southampton, UK, [3]National Oceanographic Centre, Southampton, UK, [4]University of Hamburg, Hamburg, Germany, [5]Kiewit, Inc, Omaha, NE, USA

Key Points:

- Seafloor instruments settle in sediment and new A-0-A self-calibrating pressure recorders quantify these effects
- We use Terzaghi's consolidation theory to model and correct the pressure records for settling
- The A-0-A settling corrections bring the pressure records at two sites 24 km apart to within 1 cm water depth equivalent of each other

Supporting Information:

Supporting Information may be found in the online version of this article.

Correspondence to:

N. Harmon,
nicholas.harmon@whoi.edu

Citation:

Harmon, N., Rychert, C. A., Moat, B., Smeed, D., Frajka-Williams, E., Petit, T., et al. (2026). Implications for oceanographic and seafloor geodetic applications due to settling of self-calibrating bottom pressure recorders. *Geophysical Research Letters*, *53*, e2025GL117927. https://doi.org/10.1029/2025GL117927

Received 1 JUL 2025
Accepted 11 DEC 2025

Author Contributions:

Conceptualization: Nicholas Harmon, Catherine A. Rychert, Ben Moat, David Smeed, Eleanor Frajka-Williams, Tillys Petit
Formal analysis: Nicholas Harmon
Funding acquisition: Catherine A. Rychert
Methodology: Nicholas Harmon, Martin Walker, Paul Provost, Tina Thomas
Validation: Nicholas Harmon
Writing – original draft: Nicholas Harmon, Catherine A. Rychert, Ben Moat, David Smeed, Eleanor Frajka-Williams, Tillys Petit, Martin Walker, Paul Provost, Tina Thomas
Writing – review & editing: Nicholas Harmon

© 2025. The Author(s).
This is an open access article under the terms of the Creative Commons Attribution License, which permits use, distribution and reproduction in any medium, provided the original work is properly cited.

Abstract Ocean bottom pressure recordings are a key observation for both ocean circulation and seafloor geodesy. New self-calibrating instruments may solve a long-time issue of instrument drift, allowing new high precision observations. However, instruments on the seafloor may settle over days to months, potentially contaminating results. Here we present evidence for likely settling of two self-calibrating instruments deployed along the RAPID mooring array, on the order of 8–14 cm. Settling is expected, and we model the settling based on Terzaghi's consolidation theory, which is well known in civil engineering applications. After the settling correction the difference between the two pressure records has a standard deviation of ∼1 cm water height equivalent. Settling is likely an important factor that should be considered in oceanographic and geodetic experimental design. We recommend longer term deployments of 5–10 years to allow for settling and/or selection of sites with thinner sandy sediments to minimize settling.

Plain Language Summary Measurements of the pressure at the bottom of the oceans are useful for understanding ocean currents and vertical motions of the seafloor caused by plate tectonics in earthquake prone and volcanically active regions. A new generation of bottom pressure recorders (BPR) are highly precise, meaning repeated measurements are very consistent. This allows detection of cm-scale changes in water depth. The new instruments solve a long-standing problem of long-term drift in BPR where the pressure measurement exponentially increases or decreases over periods of days to months. The new instruments will help to make advances in both oceanography and vertical geodesy used to study plate tectonic motions, through stable long-term observations. We present results from these new BPR deployed offshore the Bahamas and demonstrate their capabilities. However, they also sink and settle into the soft sediments of the seafloor over the first few months of deployment. We present a means of quantifying the settling and correcting the pressure records for the settling so that they can be analyzed for oceanographic purposes. This correction is an important step for full utilization of this data for future studies.

1. Introduction

Ocean bottom pressure is a fundamental observation for both oceanographic (Hughes et al., 2018; Williams et al., 2015; Worthington et al., 2019) and vertical seafloor geodetic purposes (Chadwick et al., 2006; Fox, 1993). Bottom pressure recorders (BPR) observe pressure changes associated oceanographic phenomena such tides, internal waves, and ocean circulation. Spatial gradients in pressure are needed for geostrophic calculations to determine current velocities and reference velocities for thermal-wind calculations based on seawater-density. For seafloor geodetic purposes, vertical motions that change the depth of the seafloor beneath a BPR are recorded as changes in pressure. Geodetic measurements using BPR have been used to measure slow slip earthquakes on the seafloor in subduction zones (Ito et al., 2013; Wallace et al., 2016), as well as volcanic inflation prior to seamount eruptions (Chadwick et al., 2006; Fox, 1993), which are both essential from a hazards perspective.

Yet, BPRs typically exhibit an initially exponential drift followed by a linear drift, overall up to several cm water-depth equivalent per year (Watts & Kontoyiannis, 1990). This drift can distort geostrophic current estimates or obscure low-frequency ocean signals (Johns et al., 2005), and it impairs detection of long-term vertical land motion critical for studying glacial isostatic adjustment and subsidence due to loading for example, cities and deltas (Herrera-García et al., 2021; Whitehouse, 2018; Wu et al., 2022). To ameliorate this issue, several methods

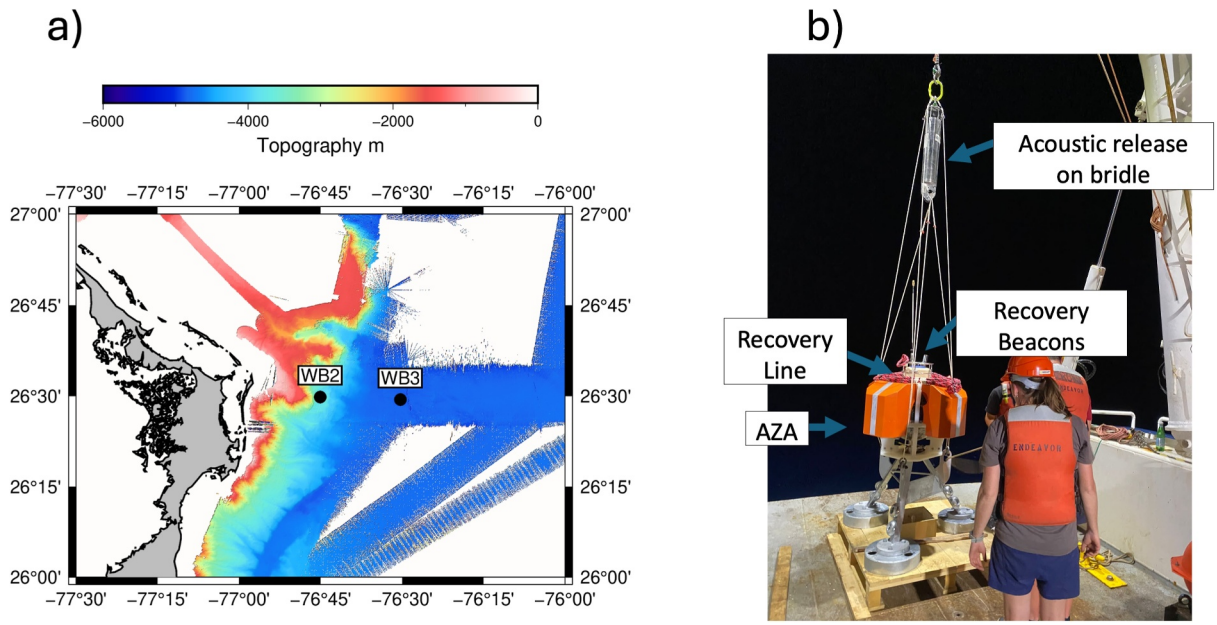

Figure 1. Map of station locations and deployment setup for the AZA. (a) Station locations for WB2 and WB3 and high resolution bathymetry of the study region (NOAA, 2024). (b) Deployment setup for the AZA showing the stand used for the instruments and recovery aides.

have been developed to calibrate the records, for example, using a dead-weight system (Sasagawa & Zumberge, 2013), or calibrating against a reference system via a remotely operated vehicle that is regularly deployed (Chadwick et al., 2006). Alternatively, pressure sensors can be calibrated at regular intervals against an internal chamber held at atmospheric pressure, known as the A-0-A calibration (Kajikawa & Kobata, 2019; Wilcock et al., 2021). The advantage of this approach is that no additional ship time or equipment are needed for the calibration. The technology is relatively new, but initial results have shown it is effective (Kajikawa & Kobata, 2019; Wilcock et al., 2021).

Another challenge for BPR use in oceanography and vertical seafloor geodesy is that the solid Earth and oceans generate signals that may contaminate each other. Typically oceanographic studies use BPRs for shorter term phenomena (<1 year) due to the drift and assume that there is no vertical motion of the seafloor (Hughes et al., 2018). This assumption is fine for most locations on Earth, but is tenuous in active tectonic regions or where significant loading of the seafloor or resource extraction occur (Thomas et al., 2024). For geodetic purposes, much work has been devoted toward disentangling oceanographic effects from seafloor motions. Reference stations are used to subtract out oceanographic effects from geodetic BPR arrays (Ito et al., 2013; Wallace et al., 2016; Watts et al., 2021; Woods et al., 2022), assuming that oceanographic effects are coherent across the array, while the reference station is geodetically stationary. Oceanographic models (Muramoto et al., 2019; Woods et al., 2022), statistical analysis and altimetric and oceanographic data (Fredrickson et al., 2023; Gomberg et al., 2019; Watts et al., 2021) have also been used to reduce the effects of oceanographic phenomena and highlighted cm-scale vertical motions in BPR data. Another approach is to deploy the BPRs adjacent to moorings, to assess the changes in the water column directly (Williams et al., 2015).

The RAPID/MOCHA tall mooring array was designed to study the changes in the Atlantic Meridional Ocean Circulation at 26°N from the Bahamas to the Canary Islands (Srokosz, 2003). The array has been in operation since 2004 and includes full water depth moorings along the western boundary measuring pressure, temperature, salinity, and velocity alongside standard BPRs, that suffer from drift. Two high precision Sonardyne Fetch AZA BPRs with the A-0-A correction (hereafter AZA) were deployed alongside moorings on the western boundary of the RAPID/MOCHA array offshore the Bahamas (Figure 1a). We demonstrate the A-0-A corrections for the pressure measurements. The instruments are located on old >175 Myr old seafloor (Muller et al., 2008), which is likely substantially sedimented. So we also investigate instrument subsidence due to sediment compaction and present a model for compaction to correct for this effect. We evaluate the precision of the instruments relative to each other, and we discuss the implications of potential settling for future experiments using AZAs.

19448007, 2026, 1, Downloaded from https://agupubs.onlinelibrary.wiley.com/doi/10.1029/2025GL117927 by NICE, National Institute for Health and Care Excellence, Wiley Online Library on [03/01/2026]. See the Terms and Conditions (https://onlinelibrary.wiley.com/terms-and-conditions) on Wiley Online Library for rules of use; OA articles are governed by the applicable Creative Commons License

19448007, 2026, 1, Downloaded from https://agupubs.onlinelibrary.wiley.com/doi/10.1029/2025GL117927 by NICE, National Institute for Health and Care Excellence, Wiley Online Library on [03/01/2026]. See the Terms and Conditions (https://onlinelibrary.wiley.com/terms-and-conditions) on Wiley Online Library for rules of use; OA articles are governed by the applicable Creative Commons License

2. Methods

The western boundary component of the RAPID/MOCHA array includes two full water depth moorings at ~3,800 m water depth at site WB2 and 4,800 m water depth at site WB3 (Figure 1a). The AZAs were deployed within 1 km of the RAPID/MOCHA array moorings on separate platforms with steel tripod stands (Figure 1b) in February 2023 aboard the RV Endeavor. Data was telemetered from the AZAs in December 2024 after ~21 months. The AZA at WB2 experienced power issues and was recovered. The AZAs sampled bottom pressure, internal instrument temperature, tilt of the instrument in two components and inverted echo sounder two-way travel time measurements hourly. The A-0-A calibration was performed with a sliding schedule; every 2 days in the beginning, transitioning to every 12 days over the course of the deployment.

AZA systems have three pressure sensors; an internal barometer kept in an internal chamber near atmospheric pressure (~100 kPa or for reference to pressure units traditionally used in oceanography 10 dbar), a Keller pressure sensor that measures ambient seafloor pressure, and a Paros Scientific Digiquartz pressure sensor that is used for the A-0-A calibration that switches between both the ambient seafloor pressure and the internal chamber pressure. The difference between the internal barometer and the Digiquartz is used to determine the bias of the Digiquartz as a function of time, and then the bias of the Keller pressure sensor as a function of time is in principle determined relative to the Digiquartz bias. The bias of the Digiquartz determined at atmospheric pressure internally is assumed to be the same at ambient seafloor pressure. Both the Digiquartz and Keller sensors experience changes in temperature due to increased power usage during the A-0-A cycle (Figures S2 and S3 in Supporting Information S1). During the A-0-A cycle, the Digiquartz sensor may take more than one sampling interval to settle to a stable ambient pressure measurement after the A-0-A cycle, whereas the Keller pressure sensor is supposed to be more stable over the A-0-A cycle.

The A-0-A correction is applied in the following way. The bias correction, δP_{corr}, for each A-0-A cycle is calculated as $\delta P_{\mathrm{corr}} = P_{\mathrm{barom}} - P_{\mathrm{digiq}}$, where P_{barom} is the internal barometer pressure and P_{digiq} is the Digiquartz internal pressure measurement for the cycle. The bias correction is then smoothed and linearly interpolated to the hourly sampling of the Digiquartz and Keller pressure records. The bias correction for the Keller pressure record uses measurements at the start of the AZA cycle when a measurement at ambient pressure is made using both the Digiquartz and Keller pressure sensors. The additional bias correction for the Keller sensor for each A-0-A cycle, $\delta P_{\mathrm{Kcorr}}$, is given by $\delta P_{\mathrm{Kcorr}} = P_{\mathrm{digiq}} - P_{\mathrm{keller}}$, where P_{keller} is the Keller pressure record. The correction is then smoothed and linearly interpolated to the hourly sampling of the Keller pressure record (Supporting Information S1). Then both interpolated corrections are then added to the hourly Keller pressure record and δP_{corr} is added to the hourly Digiquatz record. We only show records from the Digiquartz record in this paper as we found the sensor to be more stable during the AZA cycle compared to the Keller sensor (Supporting Information S1). We detide the signals using a least squares fit for the amplitude of the tidal heights predicted from the Oregon State global tidal model (Dushaw et al., 1997) and remove the mean value.

Given the likelihood that the instruments are located on sedimented seafloor, we investigate the possibility of subsidence. We use Terzaghi's 1-D consolidation theory for soil compaction (Kaliakin, 2017). The non-dimensional average subsidence U_z is given by:

$$U_Z = 1 - \sum_{n=0}^{\infty} \frac{2}{(M_n)^2} \exp\left(-M_n^2 T_v\right) \tag{1}$$

where M_n is defined as:

$$M_n = \left(n + \frac{1}{2}\right)\pi \tag{2}$$

and T_v is a function of time, t, consolidation layer thickness H_{dr} (m), and the coefficient of consolidation c_v:

$$T_v = \frac{c_v t}{(H_{\mathrm{dr}})^2} \tag{3}$$

19448007, 2026, 1, Downloaded from https://agupubs.onlinelibrary.wiley.com/doi/10.1029/2025GL117927 by NICE, National Institute for Health and Care Excellence, Wiley Online Library on [03/01/2026]. See the Terms and Conditions (https://onlinelibrary.wiley.com/terms-and-conditions) on Wiley Online Library for rules of use; OA articles are governed by the applicable Creative Commons License

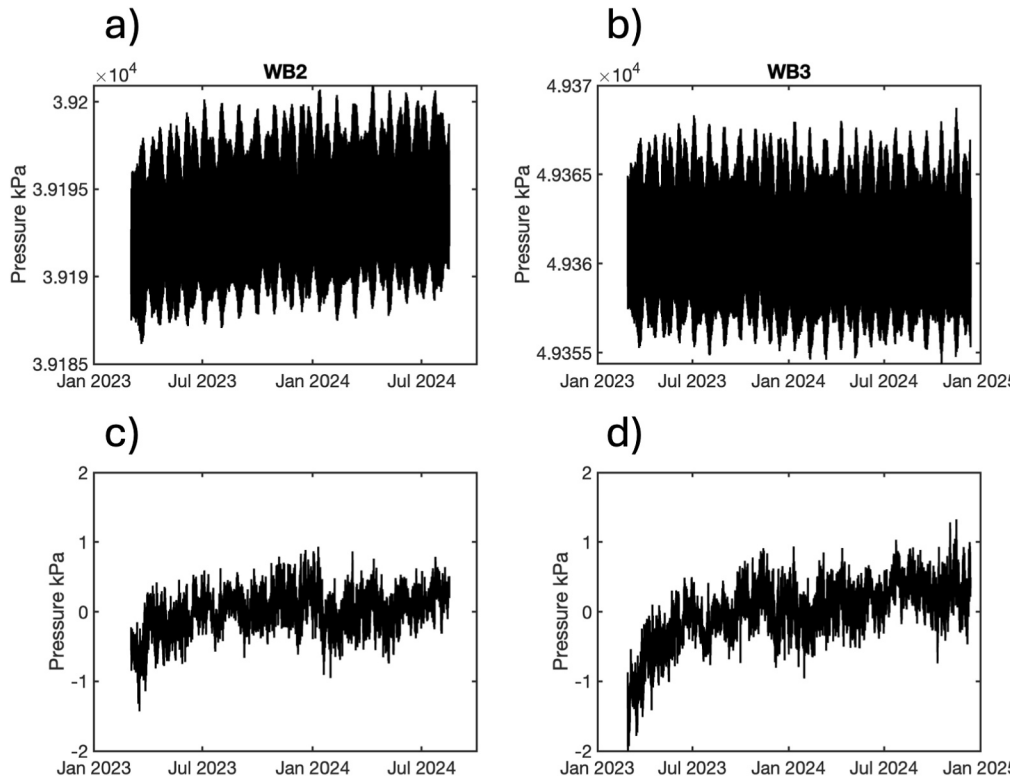

Figure 2. Time series of pressure records. Raw pressure records at sites (a) WB2 and (b) WB3. Time series of detided and AZA corrected records at sites (c) WB2 and (d) WB3.

c_v can further be expressed in terms of hydraulic conductivity, k (m/s), which describes the fluid flow of the system, unit weight of water γ_w (density × gravity, 9.81 kN m^{-3}), and coefficient of volume compressibility m_v (m^2 kN^{-1}), which describes the ratio of volume change per change in effective stress of the sediment. The denominator in Equation 4 below is also referred to as specific storage (Supporting Information S1). Volume compressibility of marine clay can range from 0.01 to 1.0 m^2 kN^{-1} (Scott & Reece, 2025), while hydraulic conductivity in marine sediments can range from 10^{-14} to 10^{-4} m/s (Shen et al., 2015).

$$c_v = \frac{k}{\gamma_w m_v}. \tag{4}$$

We first normalized the data, to have an initial mean of 0.0 over the first week and a final average value of 1 in the final 3 months of recording. T_{v0} is defined as $c_v/(H_{dr})^2$, and $(T_{v0})^{-1}$ is the characteristic time frame for the settling. We then solved Equation 1 for the best fitting T_{v0} via a line search for each normalized pressure record. We estimate hydraulic conductivity given that sediment thicknesses in our study region is much greater than the upper few meters of sediment that matter in terms of compaction (Text S2 in Supporting Information S1) and the typical range of coefficients of volume compressibility. Alternatively, the ranges of acceptable parameters (H_{dr}, k, and m_v) could be determined using extra geologic and geophysical observations. We also note that in practice, the series in Equation 1 converges at around $n = 100$.

The instruments have 3 legs (Sonardyne, 2025), and therefore the 1-D model is only an approximation. However, 3-D modeling using a finite element approach assuming parameters consistent with ranges reported above provide a similar fit to the data, suggesting the 1-D approximation sufficiently describes the subsidence, at least to first order (Supporting Information S1).

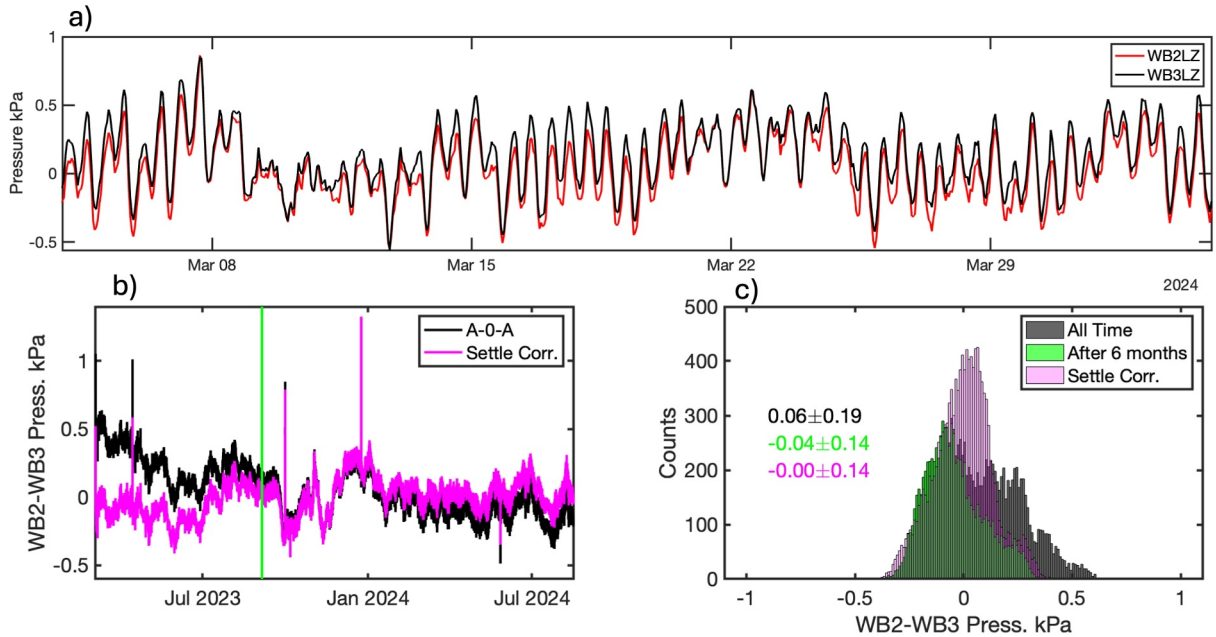

Figure 3. Comparison of two AZA pressure recordings from Site WB2 and WB3. (a) Detided and A-0-A corrected records from WB2/WB3 for March 2024, showing good agreement between the sites that are 24 km away from each other. (b) Pressure difference as a function of time showing the long-term trend due to differential settling of the instruments after A-0-A correction (Black line). Magenta line shows pressure records after settling correction. (c) Histograms of pressure difference, black all time for A-0-A corrected records, green for the period after 03 September 2023 (∼6 months from start), and magenta for the settling corrected data. Mean and standard deviation are given in the corresponding colors.

3. Results

Raw pressure signals from WB2 and WB3 are dominated by tidal signals (Figures 2a and 2b). The mean of the raw WB2 record is 39,193.22 kPa with a range of 39,186.15–39,200.93 kPa, while the mean of the raw WB3 record is 49,360.80 kPa with a range of 49,354.37–49,368.74 kPa. There is an apparent trend in the raw WB2, while raw WB3 data exhibits very little trend. The A-0-A corrections appears exponential, with WB3 ranging from 1.72 to 4.15 kPa, and WB2 ranging from −0.71 to −3.14 kPa (Figure S4 in Supporting Information S1). After the A-0-A correction and removal of the mean and tides, the range of pressure anomaly at WB2 is −1.49 to 0.93 kPa, and the range of pressure anomaly at WB3 is −2.04 to 1.33 kPa (Figures 2c and 2d). An increase in pressure with time is visible at the beginning of both records. The rate of increasing pressure decreases with time for the first 6–10 months with an apparent exponential trend, after which both records are relatively stable. The increase in pressure observed at both stations in the drift corrected records is consistent with expectations of settling of the AZAs into soft sediments, although we cannot preclude the possibility that errors in the A-0-A correction contribute to this trend. The exponential form of records during the time of settling resembles the instrument drift observed in uncalibrated BPRs and would be difficult to distinguish without the A-0-A correction. The difference of the mean between the first 30 days of data and the last 30 days of data is 0.82 kPa for WB2 and 1.44 kPa for WB3, or ∼8 and 14 cm of depth change, respectively assuming a seawater density of 1,030 kg m^{-3} and gravity of 9.81 m/s^2.

After the A-0-A correction there is good general agreement between the pressure records at WB2 and WB3, which are 24 km apart (Figure 1a). Harmonics are still visible in the data likely related to local tides and internal waves. For the period shown in March 2024, the two records are typically within 0.1 kPa (Figure 3a). However, the difference between the two records shows a non-zero decreasing trend. The pressure difference decreases from ∼0.5 to ∼0.0 kPa from February 2023 through at least July 2023 and possibly later (Figure 3b). The histogram of the pressure difference between the two time series over the observation period shows a broad distribution, with an average of 0.06 kPa and a standard deviation of 0.19 kPa, while for the period after September 2023, the average is −0.04 kPa with a standard deviation of 0.14 kPa (Figure 3c). The broader distribution of the pressure difference for the entire time series is likely related to the different settling that occurred at the two sites. For reference, we also removed an empirical exponential/linear fit to the detided data as done in previous work

19448007, 2026, 1, Downloaded from https://agupubs.onlinelibrary.wiley.com/doi/10.1029/2025GL117927 by NICE, National Institute for Health and Care Excellence, Wiley Online Library on [03/01/2026]. See the Terms and Conditions (https://onlinelibrary.wiley.com/terms-and-conditions) on Wiley Online Library for rules of use; OA articles are governed by the applicable Creative Commons License

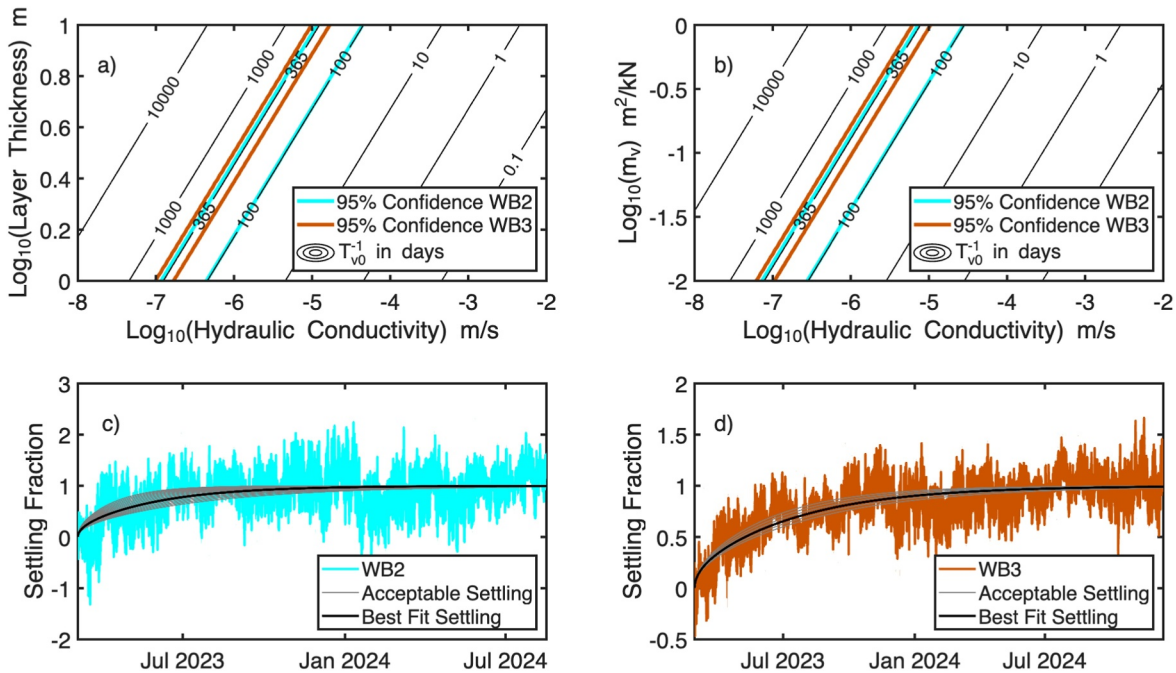

Figure 4. Modeling of settling parameters. (a) Settling time contours for different combinations of hydraulic conductivity and draining layer thickness. (b) Settling time contours for different combinations of volume compressibility (m_v) and hydraulic conductivity. (c) Model fit for WB2 and (d) model fit for WB3.

(Watts & Kontoyiannis, 1990). This approach achieves a similar average difference of 0.01 kPa with a standard deviation 0.14 kPa but does not preserve long term linear trends in the data.

We can model the increase in pressure as subsidence using Equation 1 to constrain settling parameters (Figure 4). The best fit value for $(T_{v0})^{-1}$ at WB2 is 206 days with a 95% confidence range of 109–359 days, and at WB3 it is 359 days with a 95% confidence range of 272–433 days. We note that using the first term in the summation in Equation 1, these time scales are scaled by a factor $(\pi/2)^{-2}$ or ∼0.41 which yields a shorter time scale where the largest changes occur. Visually, the best fit and fits within the confidence regions agree well with the long-term trends visible in the record from WB2 and WB3 (Figures 4c and 4d, respectively). The best fit model reduces the standard deviation of the WB2 record to 0.31 kPa, while for WB3 the standard deviation is reduced to 0.14 kPa, which is in line with the peak-to-peak differences visible in Figure 3a.

By scaling U_z to the original records and subtracting the settling, we can correct for the predicted settling at WB2 and WB3. The correction removes the linear trend in the pressure difference between WB2 and WB3 over February 2023–July 2023 (magenta line Figure 3b). The settling correction reduces the mean of the pressure difference between WB2 and WB3 to 0.00 kPa, with a standard deviation of 0.14 kPa for the entire recording period (Figure 3c).

4. Discussion

Our settling times are generally consistent with expectations from the nearest constraints on sediment properties from drilling and previous work. There are two ocean drilling holes within a few hundred kilometers of our sites with good constraints on sediment type and thickness. Ocean Drilling Project Leg 172, Hole 1062 near the Blake Bahamas Outer Ridge, has at least 320 m of nano-fossil rich clays, red lutites, and pelagic clays (Keigwin & Acton, 2001). The oldest sediments are at least 2.83 Myr old (Keigwin & Acton, 2001). Deep Sea Drilling Project Legs 52 and 102, Hole 418 near the southern end of the Bermuda Rise, has ∼320 m of sediment, with nano-fossil rich clays at the top, and deeper pelagic and zeolite rich clays with ages to the Aptian (113–121 Myr ago) (Parties, 1980; Party, 1986). Based on this information, we assume that the consolidating sediment thickness is at most ∼300 m in our region. In reality, only the top few meters are likely the consolidating layer based on our 3-D modeling (Supporting Information S1). Assuming the consolidating layer is <10 m and volume compressibility is between 0.01 and 1.0 m^2 kN^{-1} (Vivekananda & Nagaraj, 2025), the hydraulic conductivities are likely within the

19448007, 2026, 1, Downloaded from https://agupubs.onlinelibrary.wiley.com/doi/10.1029/2025GL117927 by NICE, National Institute for Health and Care Excellence, Wiley Online Library on [03/01/2026]. See the Terms and Conditions (https://onlinelibrary.wiley.com/terms-and-conditions) on Wiley Online Library for rules of use; OA articles are governed by the applicable Creative Commons License

range of 10^{-7}–10^{-5} m/s given our 95% confidence regions for WB2 and WB3, but could extend to lower values of 10^{-8} if consolidating layers <1 m are considered. The range of hydraulic conductivities is in good general agreement with the range of hydraulic conductivities for clayey soils 10^{-14}–10^{-7} m/s based on pore size arguments (Ren & Santamarina, 2018), and in situ measurements of marine sediments clays and silts that range from 10^{-10} to 10^{-7} m/s with higher values of 10^{-6} to 10^{-4} m/s for sandy fractions (Shen et al., 2015). This overall agreement with these sediment constraints further supports our assumption that the first 100s of days of recordings are strongly impacted by settling.

If unaccounted for, differential settling between sites can result in artifacts in oceanographic geostrophic calculations and seafloor geodetic work. Geostrophic calculations require accurate pressure differences between sites to determine reference velocities and could be mapped as year-long anomalies. This may lead to disagreement between mooring-based estimates for ocean circulation and BPRs. For vertical seafloor geodesy, using reference station methods (e.g., Wallace et al., 2016), the differences in settling could be mapped into apparent seafloor motions and/or affect the uncertainty of the estimates. Finally, for acoustic-GNSS horizontal motion techniques, which utilizes the centroid of small arrays of seafloor transponders, differential settling between transponders could be mapped into spurious horizontal motions. Specifically, changes in depth of a few cm between the transponders could be mapped into horizontal motions of the array of a similar order, and may explain why the first year of acoustic-GNSS measurements are not as stable as subsequent years in terms of long term plate motions (Nishimura et al., 2014; Spiess et al., 1998). However, there are several approaches that can be taken to avoid contamination related to settling.

Based on the consolidation model presented here, geological/geophysical information can be used to guide AZA site location choices to minimize settling times and to model settling a posteriori. Specifically, seismic or drill core constraints on consolidating layer thickness, the coefficient of compressibility, volume compressibility, and/or hydraulic conductivity can be used to estimate settling times via Equations 1–3. 3-D modeling (Supporting Information S1) can be used with information about the weight of the instrument and footprint to estimate the order of magnitude of compaction and duration, although we have demonstrated the 1-D solution provides a sufficient description of the subsidence.

The 1-D model provides general insights. Figure 4a illustrates the trade-offs for $T_{v0}{}^{-1}$ for consolidating layer thickness and hydraulic conductivity for a given m_v of 0.4 m^2 kN^{-1} and Figure 4b illustrates the trade-offs for m_v versus hydraulic conductivity for a fixed H_{dr} of 5 m. For a given hydraulic conductivity, sites with thinner sediment layers have shorter settling times. Sandier sediments have higher hydraulic conductivities and will have shorter settling times than clayey soil types. Higher volume compressibility in marine clays will also produce longer settling times.

Although instrument settling owing to underlying deep sedimentation is not frequently discussed in geophysical literature, its existence is well-known (Cook & DeSanto, 2019). For instance, ocean bottom seismometers are equipped with tilt meters and follow a periodic re-leveling routine to make adjustments to the orientation of their sensors as the instrument sinks (Webb et al., 2001). We also observe some correlation with the tilt records and pressure records that support settling (Figure S6 in Supporting Information S1). A previous AZA deployment used a ROV to drive the instrument into the sediment to avoid issues with subsidence (Wilcock et al., 2021). Despite this, the instrument continued to settle, first in a non-uniform way for the first 2 weeks and then by at least 0.03 kPa (3 mm) afterward (Wilcock et al., 2021). Other calibrated BPR studies were deployed on hard rock to study volcanic inflation, and therefore, should not have appreciable settling (Chadwick et al., 2006; Fox, 1993).

Given the time scale of the observed settling, long term deployment (5–10 years) of A-0-A corrected BPRs is recommended. Shorter term deployments of 1-year to 18 months are likely to be contaminated by settling in regions with substantial sediment, which includes most ocean basins. Although we have presented a means to correct for settling, uncertainty in the correction may introduce a bias on the order of 1 cm based on inspection (gray lines in Figures 4b and 4c). A conservative approach to utilizing the AZA data would be to use data only after the instrument has completely settled based on modeling.

Overall, although our study highlights the potential impact of settling on BPRs, we also demonstrated the high precision of the instruments after settling corrections were applied and/or outside the settling time. The pressure records at WB2 and WB3 are very coherent and after the A-0-A correction and the settling correction the difference between the records have a standard deviation of ∼1.4 cm water depth equivalent for the entire

19448007, 2026, 1, Downloaded from https://agupubs.onlinelibrary.wiley.com/doi/10.1029/2025GL117927 by NICE, National Institute for Health and Care Excellence, Wiley Online Library on [03/01/2026]. See the Terms and Conditions (https://onlinelibrary.wiley.com/terms-and-conditions) on Wiley Online Library for rules of use; OA articles are governed by the applicable Creative Commons License

19448007, 2026, 1, Downloaded from https://agupubs.onlinelibrary.wiley.com/doi/10.1029/2025GL117927 by NICE, National Institute for Health and Care Excellence, Wiley Online Library on [05/01/2026]. See the Terms and Conditions (https://onlinelibrary.wiley.com/terms-and-conditions) on Wiley Online Library for rules of use; OA articles are governed by the applicable Creative Commons License

overlapping period of observation (Figure 3b magenta line, Figure 3c). The two independent settling corrections remove the linear trend visible in the difference before July 2023 (Figure 3b black vs. magenta line). Some of the apparent week to month long variability between the sites may be related to physical oceanographic effects such as meso-scale and sub-meso-scale eddies, which have wavelengths on the order of the distance between the sites (Rhines, 2001). In detail, the peak-to-peak variability is on the order of ∼0.05 kPa during many time periods (sub-cm scale water depth equivalent), which suggests that the A-0-A and settling correction described here may achieve the necessary precision for fine-scale geostrophic and geodetic studies over years to decadal time scales.

5. Conclusion

BPRs on the seafloor can settle over long time periods, resulting in exponential increases in pressure with time over weeks to months, visible even after A-0-A corrections have been applied. Terzaghi's consolidation theory effectively models this settling and can be used to correct pressure data for settling. Consolidation theory along with other geologic information can constrain soil properties such as hydraulic conductivity or the coefficient of compressibility. Long term deployments of AZAs are recommended to allow time for the instrument to settle. Pre-existing geologic/geophysical knowledge of a study site may be used to select deployment locations with thinner sediments, lower volume compressibility, and/or high hydraulic conductivities that will have shorter settling times or optimized bases for AZAs can be designed. Soil properties and consolidation theory may be used to correct the pressure data but adds to the uncertainty. Unaccounted for differential settling between sites can potentially impact geostrophic estimates of currents for oceanography, vertical motion estimates from arrays of BPRs, and transponder array centroids. More detailed testing of multiple instruments at a site where sediment is minimal and tectonic motions are not expected is needed to establish effectiveness and best practices.

Conflict of Interest

The authors declare no conflicts of interest relevant to this study.

Data Availability Statement

The pressure data used for the study will be available at the RAPID data depository (Moat et al., 2025). The 3-D Terzaghi's consolidation model can be found on Zenodo (Harmon, 2025).

Acknowledgments
The authors acknowledge funding from the EU Horizon Grant 101059547 (EFW), Natural Environment Research Council NE/Y003551/1 and NE/Y005589/1 (BM and DS), and Wood Hole Oceanographic Institution (CAR and NH). Views and opinions expressed are however those of the authors only and do not necessarily reflect those of the European Union. Neither the European Union nor the granting authority can be held responsible for them. We also thank the captains and crew of the RV Endeavor and RRS Discovery.

References

Chadwick, W. W., Nooner, S. L., Zumberge, M. A., Embley, R. W., & Fox, C. G. (2006). Vertical deformation monitoring at axial seamount since its 1998 eruption using deep-sea pressure sensors. *Journal of Volcanology and Geothermal Research*, *150*(1), 313–327. https://doi.org/10.1016/j.jvolgeores.2005.07.006

Cook, M. J., & DeSanto, J. B. (2019). Validation of geodetic seafloor benchmark stability using structure-from-motion and seafloor pressure data. *Earth and Space Science*, *6*(9), 1781–1786. https://doi.org/10.1029/2019EA000623

Dushaw, B. D., Egbert, G. D., Worcester, P. F., Cornuelle, B. D., Howe, B. M., & Metzger, K. (1997). A TOPEX/POSEIDON global tidal model (TPXO.2) and barotropic tidal currents determined from long-range acoustic transmissions. *Progress in Oceanography*, *40*(1), 337–367. https://doi.org/10.1016/S0079-6611(98)00008-1

Fox, C. G. (1993). Five years of ground deformation monitoring on axial seamount using a bottom pressure recorder. *Geophysical Research Letters*, *20*(17), 1859–1862. https://doi.org/10.1029/93GL01216

Fredrickson, E. K., Gomberg, J. S., Wilcock, W. S. D., Hautala, S. L., Hermann, A. J., & Johnson, H. P. (2023). Slow slip detectability in seafloor pressure records offshore Alaska. *Journal of Geophysical Research: Solid Earth*, *128*(2), e2022JB024767. https://doi.org/10.1029/2022JB024767

Gomberg, J., Hautala, S., Johnson, P., & Chiswell, S. (2019). Separating sea and slow slip signals on the seafloor. *Journal of Geophysical Research: Solid Earth*, *124*(12), 13486–13503. https://doi.org/10.1029/2019JB018285

Harmon, N. (2025). 3-D Terzaghi's consolidation modeling for "Implications for oceanographic and seafloor geodetic applications due to settling of self-calibrating bottom pressure recorders". https://doi.org/10.5281/zenodo.17633173

Herrera-García, G., Ezquerro, P., Tomás, R., Béjar-Pizarro, M., López-Vinielles, J., Rossi, M., et al. (2021). Mapping the global threat of land subsidence. *Science*, *371*(6524), 34–36. https://doi.org/10.1126/science.abb8549

Hughes, C. W., Williams, J., Blaker, A., Coward, A., & Stepanov, V. (2018). A window on the deep ocean: The special value of ocean bottom pressure for monitoring the large-scale, deep-ocean circulation. *Progress in Oceanography*, *161*, 19–46. https://doi.org/10.1016/j.pocean.2018.01.011

Ito, Y., Hino, R., Kido, M., Fujimoto, H., Osada, Y., Inazu, D., et al. (2013). Episodic slow slip events in the Japan subduction zone before the 2011 Tohoku-Oki earthquake. *Tectonophysics*, *600*, 14–26. https://doi.org/10.1016/j.tecto.2012.08.022

Johns, W. E., Kanzow, T., & Zantopp, R. (2005). Estimating ocean transports with dynamic height moorings: An application in the Atlantic deep western boundary current at 26°N. *Deep Sea Research Part I: Oceanographic Research Papers*, *52*(8), 1542–1567. https://doi.org/10.1016/j.dsr.2005.02.002

Kajikawa, H., & Kobata, T. (2019). Evaluation and correction for long-term drift of hydraulic pressure gauges monitoring stable and constant pressures. *Measurement*, *134*, 33–39. https://doi.org/10.1016/j.measurement.2018.10.051

Kaliakin, V. N. (2017). Chapter 9 - Example problems related to time rate of consolidation. In V. N. Kaliakin (Ed.), *Soil mechanics* (pp. 377–418). Butterworth-Heinemann. https://doi.org/10.1016/B978-0-12-804491-9.00009-4

Keigwin, L. D., & Acton, G. D. (Eds.). (2001). An overview of leg 172 literature. (Vol. 172). *Ocean drilling program*. https://doi.org/10.2973/odp.proc.sr.172.208.2001

Moat, B. I., Smeed, D. A., Rayner, D., Johns, W. E., Smith, R., Volkov, D., et al. (2025). *Atlantic meridional overturning circulation observed by the RAPID-MOCHA-WBTS (RAPID-meridional overturning circulation and heatflux array-western boundary time series) array at 26N from 2004 to 2023*. Natural Environment Research Council. https://doi.org/10.5285/33826d6e-801c-b0a7-e063-7086abc0b9db

Muller, R. D., Sdrolias, M., Gaina, C., & Roest, W. R. (2008). Age, spreading rates, and spreading asymmetry of the world's ocean crust. *Geochemistry, Geophysics, Geosystems*, *9*(4), Q04006. https://doi.org/10.1029/2007gc001743

Muramoto, T., Ito, Y., Inazu, D., Wallace, L., Hino, R., Suzuki, S., et al. (2019). Seafloor crustal deformation on ocean bottom pressure records with nontidal variability corrections: Application to Hikurangi margin, New Zealand. *Geophysical Research Letters*, *46*(1), 303–310. https://doi.org/10.1029/2018GL080830

Nishimura, T., Sato, M., & Sagiya, T. (2014). Global positioning system (GPS) and GPS-acoustic observations: Insight into slip along the subduction zones around Japan. *Annual Review of Earth and Planetary Sciences*, *42*(1), 653–674. https://doi.org/10.1146/annurev-earth-060313-054614

NOAA. (2024). National centers for environmental information.

Parties, S. S. (1980). Site 418. In *Deep sea drilling project, initial reports* (Vol. 52). https://doi.org/10.2973/dsdp.proc.515253.103.1980

Party, S. S. (1986). 3. Site 418: Bermuda rise. *Initial Report of the Ocean Drilling Project*, *102*, 95–150. https://doi.org/10.2973/odp.proc.ir.102.103.1986

Ren, X. W., & Santamarina, J. C. (2018). The hydraulic conductivity of sediments: A pore size perspective. *Engineering Geology*, *233*, 48–54. https://doi.org/10.1016/j.enggeo.2017.11.022

Rhines, P. B. (2001). Mesoscale eddies. In J. H. Steele (Ed.), *Encyclopedia of ocean sciences* (pp. 1717–1730). Academic Press. https://doi.org/10.1006/rwos.2001.0143

Sasagawa, G., & Zumberge, M. A. (2013). A self-calibrating pressure recorder for detecting seafloor height change. *IEEE Journal of Oceanic Engineering*, *38*(3), 447–454. https://doi.org/10.1109/JOE.2012.2233312

Scott, W., & Reece, J. S. (2025). The influence of diatoms on hydromechanical properties of marine sediments. *Geochemistry, Geophysics, Geosystems*, *26*(4), e2024GC012064. https://doi.org/10.1029/2024GC012064

Shen, S.-L., Wang, J.-P., Wu, H.-N., Xu, Y.-S., Ye, G.-L., & Yin, Z.-Y. (2015). Evaluation of hydraulic conductivity for both marine and deltaic deposits based on piezocone testing. *Ocean Engineering*, *110*, 174–182. https://doi.org/10.1016/j.oceaneng.2015.10.011

Sonardyne, I. (2025). *Sonardyne fetch AZA specificiations*. Sonardyne, Inc. Retrieved from https://www.sonardyne.com/wp-content/uploads/2025/01/Sonardyne_8306_AZA-Fetch.pdf

Spiess, F. N., Chadwell, C. D., Hildebrand, J. A., Young, L. E., Purcell, G. H., & Dragert, H. (1998). Precise GPS/acoustic positioning of seafloor reference points for tectonic studies. *Physics of the Earth and Planetary Interiors*, *108*(2), 101–112. https://doi.org/10.1016/S0031-9201(98)00089-2

Srokosz, M. A. (2003). Rapid climate change: Scientific challenges and the new NERC programme. *Philosophical Transactions of the Royal Society of London. Series A: Mathematical, Physical and Engineering Sciences*, *361*(1810), 2061–2078. https://doi.org/10.1098/rsta.2003.1243

Thomas, F., Livio, F. A., Ferrario, F., Pizza, M., & Chalaturnyk, R. (2024). A review of subsidence monitoring techniques in offshore environments. *Sensors*, *24*(13), 4164. https://doi.org/10.3390/s24134164

Vivekananda, K. S., & Nagaraj, H. B. (2025). Predicting coefficient of volume compressibility of fine-grained soils using appropriate soil type and soil state parameters. *Scientific Reports*, *15*(1), 1686. https://doi.org/10.1038/s41598-025-85345-z

Wallace, L. M., Webb, S. C., Ito, Y., Mochizuki, K., Hino, R., Henrys, S., et al. (2016). Slow slip near the trench at the Hikurangi subduction zone, New Zealand. *Science*, *352*(6286), 701–704. https://doi.org/10.1126/science.aaf2349

Watts, D. R., & Kontoyiannis, H. (1990). Deep-ocean bottom pressure measurement: Drift removal and performance. *Journal of Atmospheric and Oceanic Technology*, *7*(2), 296–306. https://doi.org/10.1175/1520-0426(1990)007<0296:DOBPMD>2.0.CO;2

Watts, D. R., Wei, M., Tracey, K. L., Donohue, K. A., & He, B. (2021). Seafloor geodetic pressure measurements to detect shallow slow slip events: Methods to remove contributions from ocean water. *Journal of Geophysical Research: Solid Earth*, *126*(4), e2020JB020065. https://doi.org/10.1029/2020JB020065

Webb, S. C., Deaton, T. K., & Lemire, J. C. (2001). A broadband ocean-bottom seismometer system based on a 1-Hz natural period geophone. *Bulletin of the Seismological Society of America*, *91*(2), 304–312. https://doi.org/10.1785/0120000110

Whitehouse, P. L. (2018). Glacial isostatic adjustment modelling: Historical perspectives, recent advances, and future directions. *Earth Surface Dynamics*, *6*(2), 401–429. https://doi.org/10.5194/esurf-6-401-2018

Wilcock, W., Manalang, D., Ek, F., Harrington, M., Cram, G., Tilley, J., et al. (2021). A thirty-month seafloor test of the A-0-A method for calibrating pressure gauges. *Frontiers in Earth Science*, *8*, 600671. https://doi.org/10.3389/feart.2020.600671

Williams, J., Hughes, C. W., & Tamisiea, M. E. (2015). Detecting trends in bottom pressure measured using a tall mooring and altimetry. *Journal of Geophysical Research: Oceans*, *120*(7), 5216–5232. https://doi.org/10.1002/2015jc010955

Woods, K., Webb, S. C., Wallace, L. M., Ito, Y., Collins, C., Palmer, N., et al. (2022). Using seafloor geodesy to detect vertical deformation at the Hikurangi subduction zone: Insights from self-calibrating pressure sensors and ocean general circulation models. *Journal of Geophysical Research: Solid Earth*, *127*(12), e2022JB023989. https://doi.org/10.1029/2022JB023989

Worthington, E. L., Frajka-Williams, E., & McCarthy, G. D. (2019). Estimating the deep overturning transport variability at 26 degrees N using bottom pressure recorders. *Journal of Geophysical Research: Oceans*, *124*(1), 335–348. https://doi.org/10.1029/2018jc014221

Wu, P.-C., Wei, M., & D'Hondt, S. (2022). Subsidence in coastal cities throughout the world observed by InSAR. *Geophysical Research Letters*, *49*(7), e2022GL098477. https://doi.org/10.1029/2022GL098477

19448007, 2026, 1, Downloaded from https://agupubs.onlinelibrary.wiley.com/doi/10.1029/2025GL117927 by NICE, National Institute for Health and Care Excellence, Wiley Online Library on [03/01/2026]. See the Terms and Conditions (https://onlinelibrary.wiley.com/terms-and-conditions) on Wiley Online Library for rules of use; OA articles are governed by the applicable Creative Commons License